AD-A104 562 PENNSYLVANIA STATE UNIV UNIVERSITY PARK APPLIED RESE--ETC F/G 20/4
CORRECTING FOR THE SIDEWALL BOUNDARY LAYER IN SUBSONIC TWO-DIME--ETC(U)
AUG 81 A L TREASTER, P P JACOBS, G B GURNEY N00024-79-C-6043
UNCLASSIFIED ARL/PSU/TM-81-176 NL

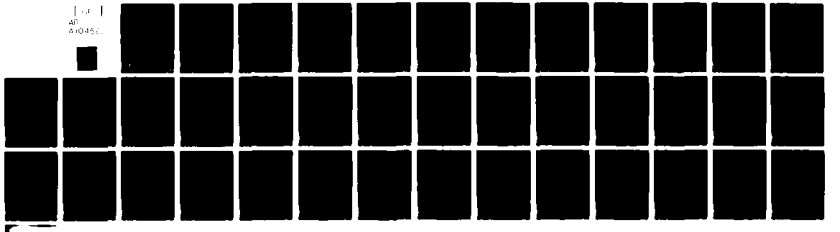

END
DATE FILMED
0 81
DTIC

CORRECTING FOR THE SIDEWALL BOUNDARY LAYER IN SUBSONIC TWO-DIMENSIONAL AIRFOIL/HYDROFOIL TESTING

A. L. Treaster, P. P. Jacobs, Jr., and G. B. Gurney

Technical Memorandum
File No. 81-176
25 August 1981
Contract No. N00024-79-C-6043

Copy No. 18

The Pennsylvania State University
APPLIED RESEARCH LABORATORY
Post Office Box 30
State College, PA 16801

Approved for Public Release
Distribution Unlimited

NAVY DEPARTMENT

NAVAL SEA SYSTEMS COMMAND

SECURITY CLASSIFICATION OF THIS PAGE (When Data Entered)

REPORT DOCUMENTATION PAGE

READ INSTRUCTIONS BEFORE COMPLETING FORM

1. REPORT NUMBER: 81-176

2. GOVT ACCESSION NO.: AD-A104 562

3. RECIPIENT'S CATALOG NUMBER:

4. TITLE (and Subtitle): CORRECTING FOR THE SIDEWALL BOUNDARY LAYER IN SUBSONIC TWO-DIMENSIONAL AIRFOIL/HYDROFOIL TESTING.

5. TYPE OF REPORT & PERIOD COVERED: Technical Memorandum

6. PERFORMING ORG. REPORT NUMBER:

7. AUTHOR(s): A. L. Treaster, P. P. Jacobs, Jr., and G. B. Gurney

8. CONTRACT OR GRANT NUMBER(s): N00024-79-C-6043

9. PERFORMING ORGANIZATION NAME AND ADDRESS:
Applied Research Laboratory
Post Office Box 30
State College, PA 16801

10. PROGRAM ELEMENT, PROJECT, TASK AREA & WORK UNIT NUMBERS:

11. CONTROLLING OFFICE NAME AND ADDRESS:
Naval Sea Systems Command
Washington, DC 20362
(Code NSEA-63R31)

12. REPORT DATE: 25 August 1981

13. NUMBER OF PAGES: 34

14. MONITORING AGENCY NAME & ADDRESS (if different from Controlling Office):

15. SECURITY CLASS. (of this report): UNCLASSIFIED

15a. DECLASSIFICATION/DOWNGRADING SCHEDULE:

16. DISTRIBUTION STATEMENT (of this Report)

Approved for public release. Distribution unlimited.
Per NAVSEA - September 3, 1981.

17. DISTRIBUTION STATEMENT (of the abstract entered in Block 20, if different from Report)

18. SUPPLEMENTARY NOTES

19. KEY WORDS (Continue on reverse side if necessary and identify by block number)

sidewall, boundary layer, correction, airfoil, hydrofoil, tests

20. ABSTRACT (Continue on reverse side if necessary and identify by block number)

Historically, two-dimensional airfoil or hydrofoil section characteristics have been obtained by measuring individually the lift, drag and pitching moment by the most accurate technique available. The use of force balances to measure the three quantities simultaneously has met with only partial success. Although the lift and pitching moment data have usually been acceptable, the drag data have varied by as much as an order of magnitude from the accepted NACA reference data. To investigate the parameters which influence two-dimensional force measurement and force balance design, an experimental program was conducted in

DD FORM 1 JAN 73 1473 EDITION OF 1 NOV 65 IS OBSOLETE

SECURITY CLASSIFICATION OF THIS PAGE (When Data Entered)

20. the subsonic wind tunnel of the Applied Research Laboratory at the Pennsylvania State University (ARL/PSU). From the results of this test program the sidewall boundary layer was identified as the primary factor contributing to the erroneous drag measurements. A correction procedure which is based on the airfoil/hydrofoil geometry, the flow environment and the measured data was developed. Corrected data from the subject test program and from similar programs in other experimental facilities for both symmetrical and cambered sections are in good agreement with NACA data in all cases.

Subject: Correcting for the Sidewall Boundary Layer in Subsonic Two-Dimensional Airfoil/Hydrofoil Testing**

Abstract: Historically, two-dimensional airfoil or hydrofoil section characteristics have been obtained by measuring individually the lift, drag and pitching moment by the most accurate technique available. The use of force balances to measure the three quantities simultaneously has met with only partial success. Although the lift and pitching moment data have usually been acceptable, the drag data have varied by as much as an order of magnitude from the accepted NACA reference data. To investigate the parameters which influence two-dimensional force measurement and force balance design, an experimental program was conducted in the subsonic wind tunnel of the Applied Research Laboratory at the Pennsylvania State University (ARL/PSU). From the results of this test program the sidewall boundary layer was identified as the primary factor contributing to the erroneous drag measurements. A correction procedure which is based on the airfoil/hydrofoil geometry, the flow environment and the measured data was developed. Corrected data from the subject test program and from similar programs in other experimental facilities for both symmetrical and cambered sections are in good agreement with NACA data in all cases.

---

*Aerodynamicist, Goodyear Aerospace Corp., Akron, OH, formerly Graduate Assistant, ARL/PSU

**This paper is being prepared for presentation at the AIAA 12th Aerodynamic Testing Conference in Williamsburg, VA, March 1982.

Acknowledgments: The authors gratefully acknowledge the technical guidance and motivational impetus supplied by Dr. B. R. Parkin, Director of the Garfield Thomas Water Tunnel, during the investigation and manuscript preparation. The authors are also indebted to the Canadian Defense Research Establishment Atlantic for the use of the drag data measured for them at CIT. The work at ARL/PSU was funded by the Naval Sea Systems Command (Code NSEA 63R31).

NOMENCLATURE

AR = aspect ratio = s^2/sc

b = exponent in Equation (11)

c = airfoil chord length

c_d = sectional drag coefficient = $D/(q_\infty \cdot s)$

c_{d_o} = sectional drag coefficient at $c_\ell = 0.0$

c_ℓ = sectional lift coefficient = $L/(q_\infty \cdot s)$

c_{ℓ_α} = local slope of the c_ℓ versus α curve

$c_{\ell_{\alpha_o}}$ = slope of the linear portion of the c_ℓ versus α curve (usually evaluated in the $c_\ell = 0.0$ region)

D = the drag force

D_e^* = Hawthorne's approximation of the energy in a secondary flow (Equation (1))

f(n) = defined by Equation (2) and Figure 12

g_i = functional operators used in developing Equation (12)

K_i = proportionality constants used in developing Equation (12)

L = the lift force

n = defined by Equation (3)

P_{ATM} = atmospheric pressure

P_s = static pressure

P_{TOTAL} = total pressure

q = local dynamic pressure = $1/2\rho u^2$

q_∞ = free stream dynamic pressure = $1/2\rho V_\infty^2$

Re = Reynolds number = $V_\infty c/\nu$

s = airfoil span

t = maximum airfoil thickness

u = local velocity

V_∞ = free stream velocity

NOMENCLATURE (Cont'd)

x = distance parallel to test section centerline measured from the leading edge of the two-dimensional test chamber

α = airfoil angle of attack

Δc_d = required correction in c_d

δ = boundary layer thickness at the balance shaft location

δ^* = boundary layer displacement thickness at the balance shaft location

ρ = mass density of the fluid

ν = kinematic viscosity of the fluid

INTRODUCTION

In the early 1970's the Applied Research Laboratory at the Pennsylvania State University, in an effort to develop new propulsor blade design criteria, attempted to measure the lift, drag and pitching moment characteristics of a hydrofoil that spanned the two-dimensional test section of the ARL/PSU 12-inch (304.8 mm) cavitation tunnel. The measurements were conducted with a three-component, cantilevered, mechanical force balance*. With the exception of the pitching moment characteristics, the data were in disagreement with accepted National Advisory Committee for Aeronautics (NACA) section data and with measurements published by other investigators. In an effort to resolve these differences and to develop a means of accurately measuring the desired hydrofoil force and moment parameters, a basic research program which was conducted by Jacobs [1]** in the ARL/PSU subsonic wind tunnel was initiated. This facility provided an environment in which the aerodynamic and geometric parameters common to both airfoil and hydrofoil testing could be easily and economically varied.

Although air and water are both fluids, fundamental differences exist in the testing requirements between the two media. Testing airfoil shapes in water (hydrofoils) introduces additional problems such as the handling of larger gross forces and waterproofing requirements. However, the major concern in water tunnel measurements is the cavitation phenomenon. A hydrofoil may operate in any or all of three different flow regimes; namely, fully wetted flow, partially cavitating flow or fully cavitating flow. Testing in fully wetted flow differs little from low-speed wind tunnel testing, and it is this regime that was of primary concern in the original ARL/PSU water tunnel test program.

A review of the literature indicated that most of the currently used NACA airfoil section data were measured in air tunnels during the 1930's and 1940's at both the Langley and Ames Research Centers. The majority of these data were acquired by measuring individually the lift, drag and pitching moment by the most accurate means available. Generally, this meant either the measurement of the pressure distributions on the ceiling and floor of the test section or the use of a force balance to obtain lift. Drag data were obtained from either wake surveys or via surface pressure distributions; a torsional balance was usually used to measure the pitching moment. Typical of these measurement programs were those conducted by Loftin and Smith [2] in 1949.

In a water tunnel, placing pressure taps on a hydrofoil surface or on the test section walls can cause premature cavitation and result in erroneous pressure measurements. At certain flow conditions, pressure probes in the profile wake are also subject to cavitation problems. For these reasons water tunnel force measurements are best performed by a mechanical force balance. With such a balance, forces can be measured directly without marring the models surface. Mechanical balances are, however, not totally free of problems. Balances measure all forces applied to a model. If forces occur on a model which are not those associated with two-dimensional flow (due to such causes as secondary

---

*In this paper a cantilevered balance refers to the experimental configuration where the model is supported from only one side of the test section and the supporting shaft is equipped with a force measuring device.

**Numbers in brackets refer to references at end of report.

flows where the model intersects a tunnel wall) the balance will also measure them. A correction procedure is then required to reduce this measured total force to a two-dimensional force. Despite the required corrections, a mechanical balance appears to be the best method for measuring forces on hydrofoils and was selected as the primary measuring instrument for the ARL/PSU wind tunnel investigation.

Other investigators have used mechanical balances for hydrofoil force measurements. Kermeen [3] used a cantilevered balance system at the California Institute of Technology (CIT) to measure forces on NACA 4412 and Walchner profile 7 hydrofoils. In correcting his data, Kermeen included the effect of tare forces and four of the traditional sources of error described by Allen and Vincenti [4]; namely, solid blockage, wake blockage, lift effect and horizontal buoyancy. Kermeen's measured lift and pitching moment data for the NACA 4412 hydrofoil were in good agreement with previous NACA data. The drag data agreed well in the lower drag range, but for angles of attack greater than five degrees Kermeen's results were nearly a factor of two higher than the NACA data as shown in Figure 1.

Earlier measurements of a similar nature were conducted by Daily [5] at CIT. Daily used a cantilevered, three-component balance which was a forerunner of Kermeen's balance to measure the forces on a NACA 4412 hydrofoil in the High-Speed Water Tunnel (HSWT). A full-span hydrofoil was used at low angles of attack; to halve the forces at higher angles of attack a split foil was used. Daily implied that his data required little correction. As with Kermeen's data the lift and pitching moment measurements were in good agreement with the NACA data. Daily was primarily interested in the low angle of attack range where the drag measurements were in good agreement with the NACA data. However, at higher angles of attack his drag measurements were approximately 50.0 percent high, Figure 2.

Since measurement of the pitching moment had not been a problem in the past, a two-component cantilevered balance was designed and fabricated for the ARL/PSU wind tunnel test program. The resulting measurements [1] produced lift data (with the traditional corrections applied) that were in agreement with NACA data, Figure 3. However, the corrected drag data, Figure 4, show differences similar to those reported by Kermeen and Daily. Subsequent pressure surveys at the midspan of the airfoil resulted in drag data that were in agreement with the reference NACA two-dimensional section data, Figure 5. After experimental study of several error sources, it was reasoned that the two-dimensionality of the flow was being altered by the presence of the sidewall boundary layer.

In wind tunnel testing the sidewall boundary layer can be controlled by blowing or suction techniques to yield the desired two-dimensional data. Because these techniques can aggravate the cavitation problem in hydrofoil testing, the alternate approach of using a correction procedure is preferred.

The independent work of Barber [6] and Hawthorne [7] relative to the secondary flows at a strut-wall intersection as a function of the incoming wall boundary layer characteristics was a starting point for the development of the desired correction procedure. Their work, when combined with an empirical parametric evaluation of the Kermeen, Daily, and ARL/PSU balance-measured drag data resulted in a correction procedure for the effects of the sidewall boundary layer that was developed by Jacobs [1] and is summarized here in Equation (12). When this correction procedure is applied to the three previously discussed sets of drag data and to additional drag data measured by Ward [8] on a NACA 16-309 hydrofoil at CIT, the results are in good agreement with NACA two-dimensional section characteristics, Figures 13, 14, and 17. Thus, based on the rather limited comparative data, it appears that a correction procedure to account for the effects of the sidewall boundary layer on balanced-measured airfoil/hydrofoil drag data has been formulated.

The specific details of the entire ARL/PSU wind tunnel test program are documented in the report by Jabobs [1]. Discussed in the remainder of this paper are the portions of the ARL/PSU test program relevant to the lift and drag measurements by the cantilevered balance, the development of the correction procedure and the application of the correction procedure to existing experimental data.

ARL/PSU WIND TUNNEL TEST PROGRAM

Test Facility and Experimental Hardware

The ARL/PSU subsonic wind tunnel in which this test program was conducted is shown schematically in Figure 6 and described in detail in Reference [9]. This facility is a closed circuit, closed jet air tunnel with a octagonal test section which is 4.0 ft (1.219 m) across the flats and is 16.0 ft (4.877 m) long. The test section velocity can be varied continuously up to 120.0 fps (36.576 m/sec). Honeycomb and screens used in the settling section reduce the turbulence level in the test section to 0.06 percent of the free-stream velocity at 80.0 fps (24.384 m/sec). For this test program two 4.0 ft x 8.0 ft (1.219 m x 2.438 m) wooden panels were mounted vertically 18.375 in (466.725 mm) apart to create a two-dimensional test section as shown in the balance installation drawing, Figure 7.

Two airfoil models of different aspect ratio, AR, were fashioned for use with the cantilever balance. A NACA 0012 airfoil was machined from aluminum. This model had a chord of 9.0 in (228.6 mm) and span of 18.375 in (466.7 mm) for an AR of 2.04. A second model was made of a two part expandable urethane foam (span = 18.375 in (466.7 mm); chord = 18 in (457.2 mm); AR = 1.02). When installed in the test chamber the airfoil was attached at its midchord to the cantilever balance. The balance shaft was located midway between the floor and ceiling of the test section and 28.0 in (711.2 mm) downstream from the leading edge of the wooden panels. Provisions were made to mount the 9.0 in (228.6) airfoil directly to the balance shaft or mounted to an 11.0 in (279. 4 mm) diameter disk on the balance shaft.

Instrumentation

The lift and drag forces were measured by a two-component, cantilevered balance that is sketched in Figure 7. This balance used the compact strain-gaged tension-member concept developed by Gurney [10]. The balance rotated with the airfoil and sensed forces normal to and parallel with the chordline. The corresponding lift and drag values were computed via standard vector resolution equations.

For the force measurements the reference velocity, V_∞, was measured by a 0.25 in (6.35 mm) diameter pitot-static probe that was located on the tunnel floor midway between the sidewalls and in the same vertical plane as the midchord of the airfoil. The probe tip was above the floor boundary layer.

Wake traverses to evaluate the drag coefficient were conducted with a 0.125 in (3.175 mm) diameter kiel probe that was located midway between the sidewalls and in a plane one chordlength downstream from the airfoils trailing edge. For these tests the reference pitot-static probe was located in the traverse plane midway between the floor and the centerline of the test section. The same kiel probe was used to make sidewall boundary layer measurements at the balance shaft location. For these measurements the reference pitot-static probe in the tunnel floor was used.

To obtain horizontal buoyancy corrections, the sidewall static pressure gradient was measured by four .032 in (.813 mm) diameter static pressure taps. Beginning 1.0 ft (304.8 mm) downstream of the sidewalls leading edge and spaced at 2.0 ft (609.6 mm) intervals thereafter. The static pressure taps were located 1.0 ft (304.8 mm) above the test section floor.

The angle of attack, α, was measured with a gunner's quadrant which was used in conjunction with an airfoil template. The template was machined so that when the template made a three-point contact with the airfoil's upper surface the top of the template was parallel to the chordline. This technique enabled the angle of attack to be measured within $\pm 0.056°$.

Based on a Student-t analysis the greatest error in the balance-measure c_ℓ values was ± 0.0038 and in c_d was ± 0.0007. A similar analysis for the c_d values obtained by the wake traverses indicated a greatest error of ± 0.00014.

Measurements and Results

The flow characteristics of the two-dimensional test section were established by a series of preliminary tests prior to the installation of the airfoil. Flow uniformity was verified for the region outside of the influence of the four test section boundary layers by kiel probe surveys. The longitudinal static pressure gradient $[(dP_s/dx)/1/2\rho V_\infty^2]$ was measured to be 0.01236 ft^{-1} (0.0406 m^{-1}). The sidewall boundary layer at the balance shaft location was measured at several Reynolds numbers; the resulting data are presented in Figure 8.

The force measurements phase with the cantilevered balance was initiated by measuring the tare forces on the 11.0 in (279.4 mm) diameter disk. For these measurements the 9.0 in (228.6 mm) airfoil was mounted on the opposite wall with a gap of 0.004 (0.102 mm) between the airfoil tip and the disk. The results are listed in Table I.

TABLE I

Disk Tare Forces*

Lift and Drag Data - Cantilevered Balance

V_∞ = 70.0 fps (21.34 m/s)

Re = 330,000

disk diameter = 11.0 in (279.4 mm)

α (deg)	c_ℓ (±0.0014)	c_d (±0.0004)
9.34	0.0094	0.0021
6.26	0.0078	0.0014
3.21	0.0055	0.0018
0.47	0.0039	0.0012
-3.43	0.0027	0.0009
-6.17	-0.0008	0.0014
-9.01	-0.0004	0.0020

*9.0 in (228.6 mm) airfoil mounted on opposite wall
coefficients nondimensionalized by c = 9.0 in (228.6 mm)

It should be noted here that to match the NACA Reynolds number conditions (Re = 330,000) the 9.0 in (228.6 mm) airfoil was tested at 70 fps (21.34 m/sec) whereas the 18.0 in (457.2 mm) airfoil was tested at 37.0 fps (11.28 m/sec).

Lift and drag were next measured for the 9.0 in (228.6 mm) airfoil while operating both with and without the disk and for the 18.0 in (457.2 mm) airfoil. The resulting c_ℓ versus α data (with the traditional corrections applied) which were judged to be in satisfactory agreement with the NACA reference data are shown in Figure 3. The corresponding drag polar is shown in Figure 4. Here the measured drag data are approximately 45.0 percent high at upper c_ℓ values. It is also interesting to observe from the data that a disk on the balance-end of the airfoil is apparently not necessary.

At this time the proven NACA approach of using separate drag measurements was attempted. The drag characteristics of the 9.0 in (228.6 mm) airfoil were measured by the downstream wake traverses at the midspan of the airfoil. The drag values were obtained by the classical procedure of integrating the wake momentum deficits. The resulting polar from the combination of the balance-measured lift data and the wake-measured drag data agreed with the NACA data, Figure 5.

What was the source of error in the balance-measured drag data? Three possible sources were considered: (1) end gap effects between the airfoil tip and the adjacent sidewall, (2) drag on the portion of the balance shaft between the sidewall and the model, and (3) contamination of the two-dimensional flow by an interaction of the airfoil and the sidewall boundary layer. The effect of the end gap between the airfoil tip and the test section wall was first investigated. Lift and drag data were measured at a constant angle of attack while varying the end gap from 0.001 in to 0.010 in (0.025 mm to 0.254 mm). For this range of end gap, no significant change in c_d was measured and less than a 1.0 percent change in c_ℓ was recorded. Parkin and Kermeen [11] reported similar results, i.e., if the end gap is sufficiently small, viscous forces predominate and the effect of the end gap is negligible.

To evaluate the drag force on the portion of the balance shaft exposed to the flow a stub spindle was fabricated. The stub spindle was mounted in the cantilevered balance and extended 0.002 in (0.508 mm) into the flow. This was the typical operating clearance at the balance end of the airfoil. The 9.0 in (228.6 mm) airfoil was mounted on the opposite wall and was maintained at a minimum distance from the spindle. Under these conditions, the flow in the vicinity of the model-sidewall intersection is closely duplicated and the balance measured only the forces on the stub spindle. The resulting data are presented in Table II.

TABLE II

Stub Spindle Drag Measurements*

V_∞ = 70.0 fps (21.34 m/sec)

Re* = 330,000

α (deg)	c_d (±0.0004)
0.00	0.0000
7.10	0.0002
7.77	0.0006
8.90	0.0008
10.80	0.0013

*9.0 in (228.6 mm) airfoil mounted on opposite wall
coefficient nondimensionalized by c = 9.0 in (228.6 mm)

Clearly the supporting shaft was not responsible for the high measured values of c_d.

Thus, only the contamination of the two-dimensional flow by the interaction of the airfoil with the sidewall boundary layer remained as a postulated cause of the erroneous drag measurement. Evidence of such an interaction was observed during the wake measurement phase where a secondary wake was measured near the sidewall, Figure 9. As previously discussed the removal of the sidewall boundary layer is not practical in water tunnel applications so that the alternate approach of developing a correction procedure was chosen.

DEVELOPMENT OF THE CORRECTION PROCEDURE

As shown in Figure 1, 2 and 4 a similar variation between balance-measured drag data and the NACA two-dimensional section characteristics existed in Kermeen's, Daily's and the ARL/PSU data. Because this difference is typical only of balance-measured data in which the entire force exerted or the airfoil/hydrofoil is measured, it was assumed that this increment in drag, Δc_d, was due to three-dimensional flow effects on the model. Such three-dimensional flow effects can be generated when a strut intersects a flat surface in the presence of a nonuniform flow. The resulting secondary flow - the so-called horseshoe vortex, Figure 10 - engulfs the strut-wall intersection and produces a region of contaminated two-dimensional flow. This type of secondary flow can be generated in airfoil/hydrofoil testing when an airfoil or hydrofoil that spans the test section intersects the test section wall in the presence of the sidewall boundary layer.

A study of this problem using flow visualization techniques was recently completed by Barber [6] in which he investigated the additional drag that is created by a strut protruding from a wall as a function of the incoming boundary layer thicknesses. He found that the size of the horseshoe vortex varied directly with the thickenss of the incoming boundary layer. He also found that the portion of the airfoil where flow separation occurred varied inversely with the size of the horse-shoe vortex. He concluded that with a large horseshoe vortex, viscous effects caused high energy fluid to be entrained in the corner where the airfoil trailing edge and wall intersects as shown in Figure 11. This influx of high energy fluid enables the flow to withstand better the adverse pressure gradient existing in the corner and, consequently, retards flow separation. As illustrated in Figure 11, a thin vortex is not able to entrain as much of the high energy fluid and a larger separated zone exists.

Hawthorne [11] derived the following expression for the energy in secondary flows, D_e^* created by strut-wall intersections:

$$D_e^* = \frac{144\, V_\infty^2\, c^2\, (t/c)^4\, f(n)}{25\, [1 + (1/2)(t/c)^2]} \quad , \qquad (1)$$

where

$$f(n) = \frac{n^2}{1+n^2}\,\frac{2}{\pi}\left\{\frac{\pi}{4n}\left(\frac{n^2-1}{n^2+1}\right)^2 + \frac{1-n^2}{(1+n^2)^2}\log_e n + \frac{1}{1+n^2}\right\} - \frac{1}{4n} \quad ; \qquad (2)$$

and

$$n = 4\,[1 + (1/2)(t/c)]/(15\pi\,\delta^*/c) \qquad (3)$$

Hawthorne's relationship between f(n) and boundary layer displacement thickness (δ^*/c) is shown in Figure 12. These data are for a bicusped strut profile in an exponential boundary layer with strut thickenss-to-chord ratios of .05 and .25. Hawthorne's figure shows that f(n) increases with δ^*/c to a maximum value at $\delta^*/c \approx 0.1$. Equation (1) states that the energy in these secondary flows is proportional to airfoil thickness to the fourth power and reaches a maximum when δ^*/c is approximately 0.1. Although the theory does not hold for all airfoil shapes or boundary layer profiles, it is probably fair to assume that generally the energy in secondary flows for this type of airfoil-tunnel wall intersection is

$$D_e^* = K_1\,(t/c)^4\,f(n) \qquad (4)$$

If the function f(n) in Figure 12 is linearized over the portion of the curve $0.0 \leq \delta^*/c \leq 0.1$, then

$$f(n) = \left[f(n)_{max}/(0.1)\right]\,(\delta^*/c) = K_2\,(\delta/c) \quad . \qquad (5)$$

In Equation (5), the momentum thickness, δ^*, has been assumed proportional to the more frequently documented boundary layer thickness, δ. Thus, D_e^* becomes

$$D_e^* = K_3\,(t/c)^4\,(\delta/c) \quad . \qquad (6)$$

Functionally, the drag correction was assumed to take the following form:

$$\Delta c_d = g_1\,(D_e^*,\ c_\ell,\ c_d,\ \alpha,\ AR) \qquad (7)$$

The inverse relationship between Δc_d and D_e^* has been established by Barber [6]. Therefore, Equation (7) can be written as

$$\Delta c_d = K_4 \frac{g_2 (c_\ell, c_d, \alpha, AR)}{(\delta/c)(t/c)^4} \tag{8}$$

The effects of c_ℓ, c_d, α and AR were derived empirically from the available experimental data.

The required Δc_d corrections for the three sets of drag data are shown by the dash-dot curves in Figures 1, 2 and 4. The three sets of data have several similarities. The deviation of drag is zero at c_ℓ=0.0 for all three investigations. The Δc_d curves for all three experiments increase to the points where c_{ℓ_α} is no longer constant and then decrease. If $c_{\ell_{\alpha_o}}$ represents the slope of the lift curve in the linear portion of the c_ℓ versus α curve, then the shape of the Δc_d versus α curve seems to vary as $[c_{\ell_\alpha}/c_{\ell_{\alpha_o}}]^{1/2}$ for all three experiments. It was assumed that this slope variation represented the angle of attack, α, contribution to the drag correction so that Δc_d can be expressed as

$$\Delta c_d = K_5 \frac{\left[c_{\ell_\alpha}/c_{\ell_{\alpha_o}}\right]^{1/2} g_3(c_\ell, c_d, AR)}{(\delta/c)(t/c)^4} \quad . \tag{9}$$

As the experimental data from the three studies show, Δc_d increases directly with c_ℓ; and Δc_d is zero at c_ℓ = 0.0. This also implies that the balances measure the correct value of c_d at c_ℓ = 0.0, namely, c_{d_o}. Thus, the c_{d_o} was included as the c_d term which "individualizes" the correction procedure to specific airfoils. When the linear dependence on c_ℓ and the c_{d_o} term are introduced in Equation (9), Δc_d becomes

$$\Delta c_d = K_6 \frac{c_\ell \cdot c_{d_o}\left[c_{\ell_\alpha}/c_{\ell_{\alpha_o}}\right]^{1/2}}{(\delta/c)(t/c)^4} g_4(AR) \tag{10}$$

The effect of aspect ratio was approximated by

$$g_4(AR) = (AR)^b \quad . \tag{11}$$

The values of K_6 and b were determined empirically from the experimental data. It was found that the best fit to the three sets of data was obtained for $K_6 = 1.5 \times 10^{-5}$ and $b = -1/2$. With the evaluation of these two constants the final form of the equation to correct the balance measured drag data for the effect of the sidewall boundary layer is

$$\Delta c_d = 1.5 \times 10^{-5} \frac{(c_\ell)(c_{do})(c_{\ell_\alpha}/c_{\ell_{\alpha_o}})^{1/2}}{(\delta/c)(t/c)^4(AR)^{1/2}} \qquad (12)$$

In summary, the proposed correction to balance-measured drag data for the effect of the sidewall boundary layer is a function of the airfoil/hydrofoil geometry (t/c and AR), the thickness of the sidewall boundary layer (δ/c), and the accurately measured balance data (c_{do} and c_ℓ versus α).

APPLICATION AND DISCUSSION

Shown in Figures 13, 14 and 15 are the results of applying the correction procedure to the Kermeen, Daily and ARL/PSU data, respectively. For Daily's half-span measurements when the balance sensed the effect of only one sidewall boundary layer, the total AR value was used but only one half of the computed Δc_d value from Equation (12) was applied to the measured data. As can be seen in these three figures the corrected drag polars are in relatively good agreement with the accepted reference data.

In practice, this correction for the sidewall boundary layer, Equation (12), is applied to the drag data after the tare readings and the traditional corrections have been applied. The technique will be illustrated by applying the procedure to data measured by Ward [8] at CIT for the Canadian Defense Research Establishment Atlantic (DREA). These data were located by the authors after the completion of Jacobs' initial studies and were not included in the development of Equation (12).

Ward used a three component, cantilevered, mechanical balance to measure lift, drag and pitching moment on a 6.0 in by 6.0 in (152.4 mm by 152.4 mm) NACA 16.309 hydrofoil in the CIT High Speed Water Tunnel. The resulting noncavitating data at 50.0 fps (15.24 m/s) with the tare corrections included are shown by the open circles in Figures 16 and 17. Also shown as solid lines in these figures are the NACA reference data (after correction for compressability effects) measured by Lindsey, et.al. [12] at a Mach number of 0.3. The data were further corrected according to Pope [13] for solid blockage, wake blockage and lift effect (streamline curvature). The sidewall of the test section was adjusted to eliminate the horizontal buoyancy effect. The results of applying these traditional corrections to the data are shown by the open squares in Figures 16 and 17. The required Δc_d correction for Wards' data is shown by the dash-dot curve in Figure 17. Again it is interesting to note that the balance has measured the correct drag value at the zero lift condition.

From Reference [8] the following parameters were obtained for the application of Equation (12):

$$c_{d_o} = 0.0009 \qquad AR = 1.00 \qquad (t/c) = 0.09$$

The c_ℓ term is, of course, the corrected lift coefficient (open squares) at each α. The $(c_{\ell_\alpha}/c_{\ell_{\alpha_o}})^{1/2}$ term was computed by fitting a differentiable mathematical spline curve through the corrected c_ℓ versus α data. Ward [14] documents the test section boundary layer characteristics at the balance shaft location of the HSWT. The average value of δ/c at 50.0 fps (15.24 m/s) is 0.108. With these values Equation (12) can now be evaluated. The resulting Δc_d values are shown as the solid squares in Figure 17. When these computed Δc_d values are applied to Ward's drag polar the corrected data are shown by the solid circles. The agreement is certainly encouraging.

CONCLUSIONS, LIMITATIONS AND RECOMMENDATIONS

The results of this ARL/PSU experimental investigation and subsequent data analysis have revealed or reaffirmed several important conclusions relative to balance-oriented, two-dimensional airfoil/hydrofoil testing:

(1) The effect of a small end gap between the airfoil tip and the channel wall is negligible provided the gap-to-chord ratio is ≤ 0.002.

(2) It was also demonstrated that the use of a flush-mounted disk at the balance-end of the airfoil is not required, at least in noncavitating flows.

(3) In the absence of the disk and for gap-to-chord ratios ≤ 0.001 the effects of flow in the region of the supporting shaft are negligible.

(4) With the application of only traditional and tare corrections, drag polars in agreement with accepted reference data can be obtained by combining the balance-measured c_ℓ values and c_d data from wake traverses.

(5) The disagreement between balance-measured drag data and the accepted reference values is primarily the result of the interaction of the airfoil and the sidewall boundary layer.

(6) The effect of the sidewall boundary layer on balance measured drag data can be accounted for by the application of Equation (12).

The previous conclusions are not without some limitations. The empirical development of Equation (12) was conducted in the absence of data obtained from studies in which there was a significant variation in aspect ratio or thickness to chord ratio. The linearized adaptation of Hawthornes f(n) - curve is only valid for $\delta^*/c \leq 0.1$. For values of $\delta^*/c > 0.1$ a different approximation of f(n) would be required. Equation (12) has been developed in terms of the boundary layer thickness measured at the balance shaft location. Since all of the subject foils were mounted at their midchord position it is not totally apparent that the midchord location is the appropriate position for the boundary layer measurements.

Obviously one of the recommendations for future study would be the acquisition of a larger data base, particularly with respect to AR

and t/c variation, for further refinement of Equation (12). The effects of the sidewall boundary layer should be further investigated by wind tunnel tests in which the horseshoe vortex can be removed by suction or blowing. And, of course, an attempt should be made to extend the proposed correction procedure to hydrofoils operating in the cavitating flow regimes.

REFERENCES

[1] Jacobs, Jr., J. J., "A Method of Correcting for the Effects of the Sidewall Boundary Layer in Two-Dimensional Airfoil Testing," The Pennsylvania State University/Applied Research Laboratory TM 80-44, March 31. 1980.

[2] Loftin, L. K., and Smith, H. A., "Aerodynamic Characteristics of 15 NACA Airfoil Sections at Seven Reynolds Numbers from 0.0×10^6 to 9.0×10^6," NACA Technical Note 1945, October 1949.

[3] Kermeen, R. W., "Water Tunnel Tests of NACA 4412 and Walchner Profile 7 Hydrofoils in Noncavitating and Cavitating Flows," California Institute of Technology, Report Number 47-5, February 1956.

[4] Allen, H. J., and Vincenti, W. G., "Wall Interference in a Two Dimensional Flow Wind Tunnel with Consideration of the Effect of Compressibility," NACA Technical Report 782, 1944.

[5] Daily, J. W., "Cavitation Characteristics and Infinite Aspect Ratio Characteristics of a Hydrofoil Section," Transactions of the ASME, Vol. 71, pp. 269-284, April 1949.

[6] Barber, T. J., "An Investigation of Strut-Wall Intersection Losses," Journal of Aircraft, Vol. 15, No. 10, pp. 676-681, October 1978.

[7] Hawthorne, W. J., "The Secondary Flow About Struts and Airfoils," Journal of the Aeronautical Sciences, Vol. 21, September 1954.

[8] Ward, T. M., "Experiments on the NACA 16-309 Foil Section Fitted with an Adjustable Flap in Fully-Wetted and Cavitating Flows," Graduate Aeronautical Laboratories, California Institute of Technology, Report HSWT-1127.

[9] Lehman, A. F., "The Garfield Thomas Water Tunnel," Serial No. NOrd 16597-56, Appendix III, pp. 66-77, September 30, 1959.

[10] Gurney, G. B., "An Analysis of Force Measurement," M. S. Thesis, The Pennsylvania State University, September 1962.

[11] Parkin, B. R., and Kermeen, R. W., "Water Tunnel Techniques for Force Measurements on Cavitating Hydrofoils," Journal of Ship Research, Vol. 1, No. 1, April 1957, p. 36.

[12] Lindsey, W. F., Stevenson, D. B. and Daley, B. N., "Aerodynamic Characteristics of 24 NACA 16-Series Airfoils at Mach Numbers Between 0.3 and 0.8," Technical Note No. 1546, Langley Aeronautical Laboratory, Langley Field, Virginia, September 1948.

[13] Pope, A., and Harper, J. J., Low Speed Wind Tunnel Testing, John Wiley and Sons, Inc., New York, 1966.

[14] Ward, T. M., "The Hydrodynamics Laboratory at the California Institute of Technology - 1976," Journal of Fluids Engineering, ASME, December 1976.

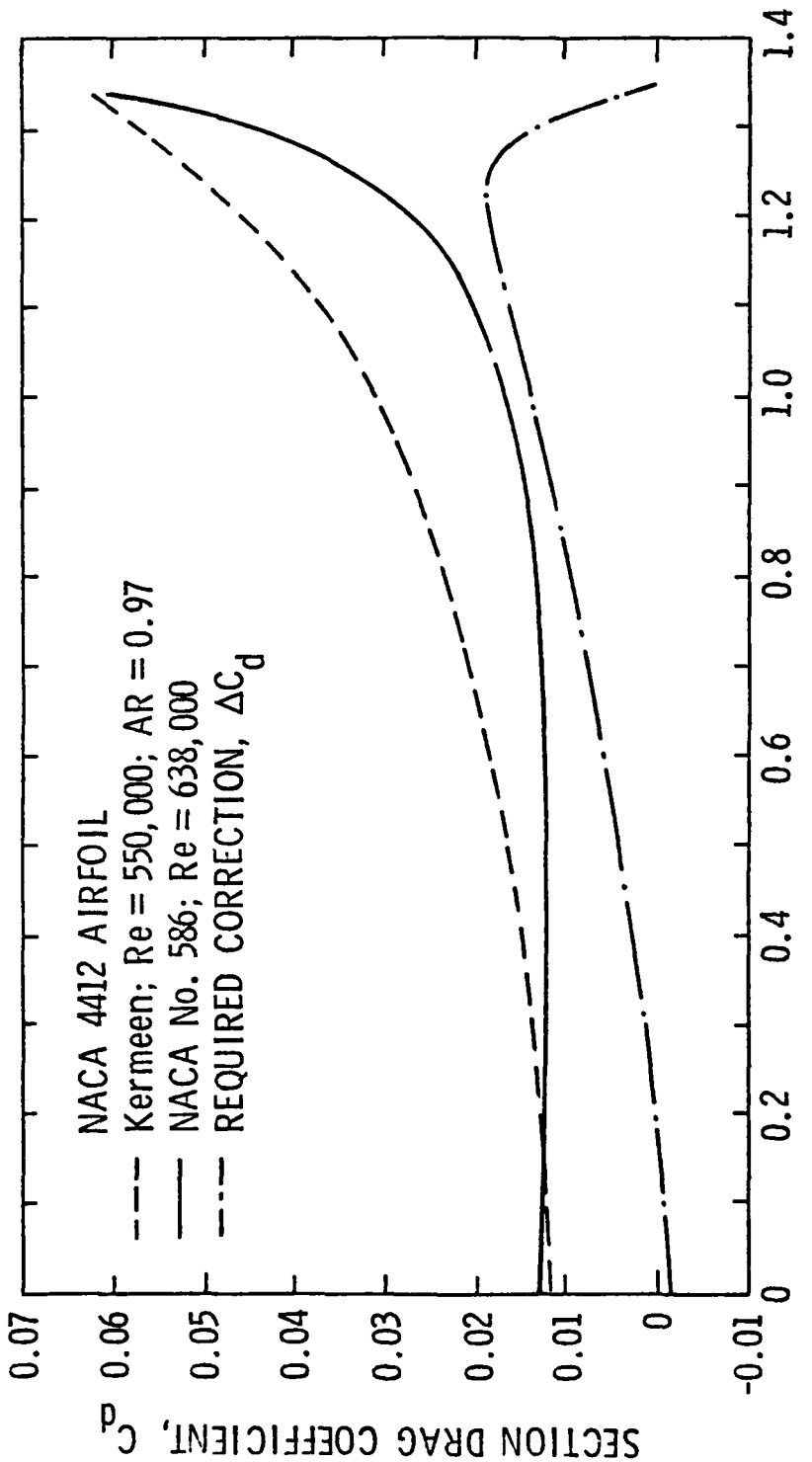

Figure 1. Kermeen's drag polar compared with NACA published data for a NACA 4412 airfoil. Also shown is the value of ΔC_d required to correct Kermeen's curve to the NACA curve.

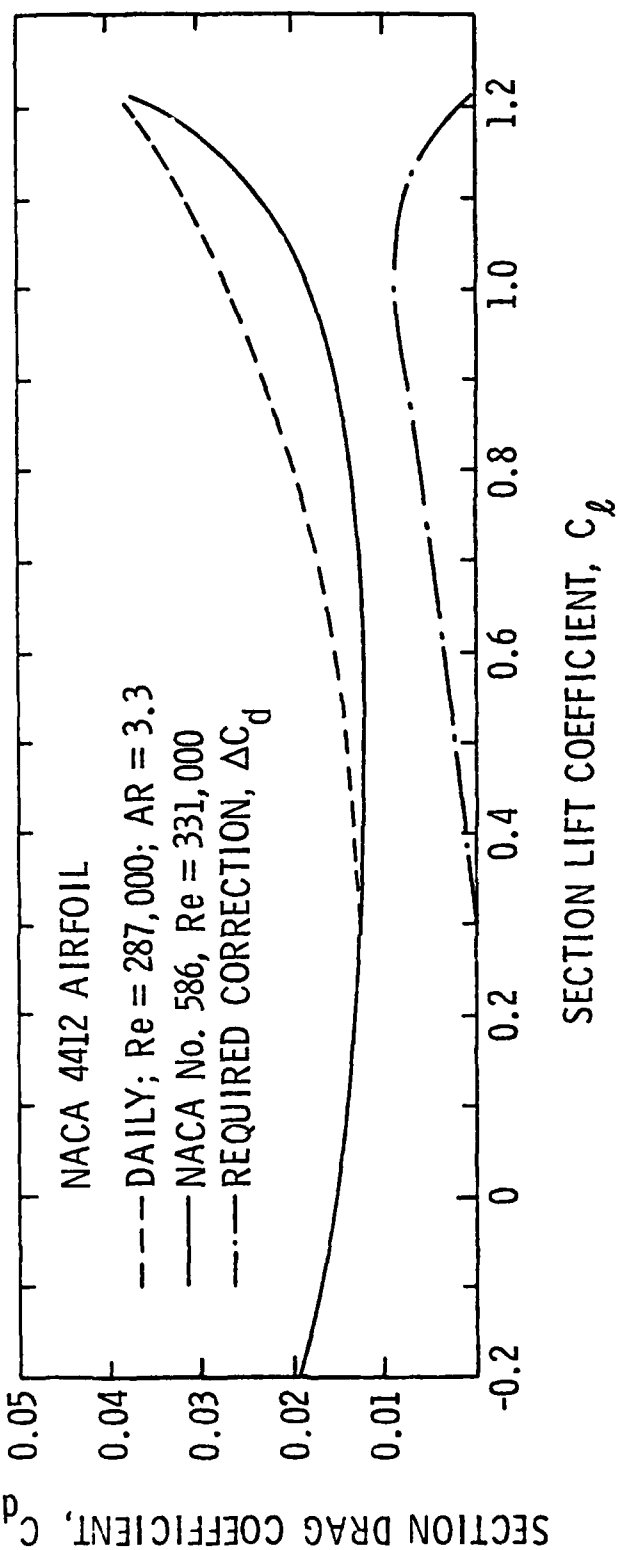

Figure 2. Daily's drag polar compared with NACA published data for a NACA 4412 airfoil. Also shown is the value of ΔC_d required to correct Daily's curve to the NACA curve.

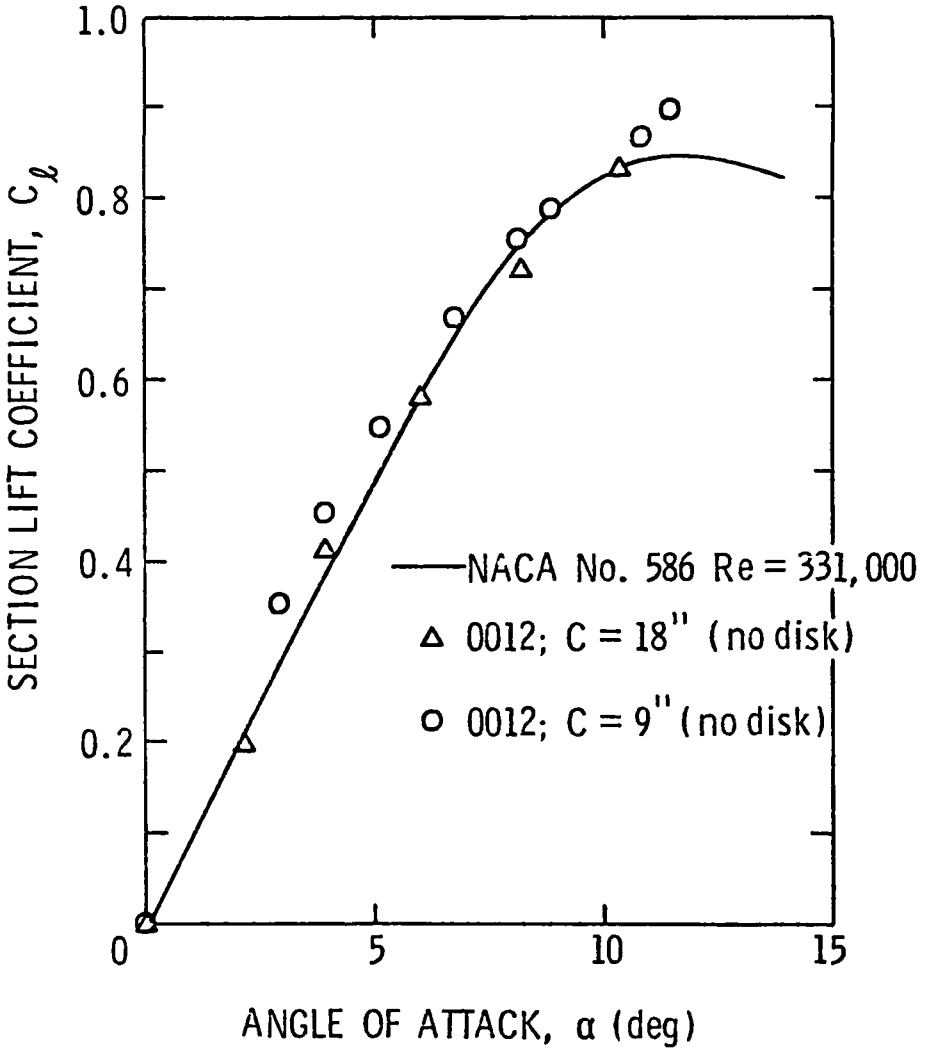

Figure 3. ARL/PSU sectional lift characteristics airfoil without disk c = 9.0 in (228.6 mm) and c = 18.0 (457.2 mm).

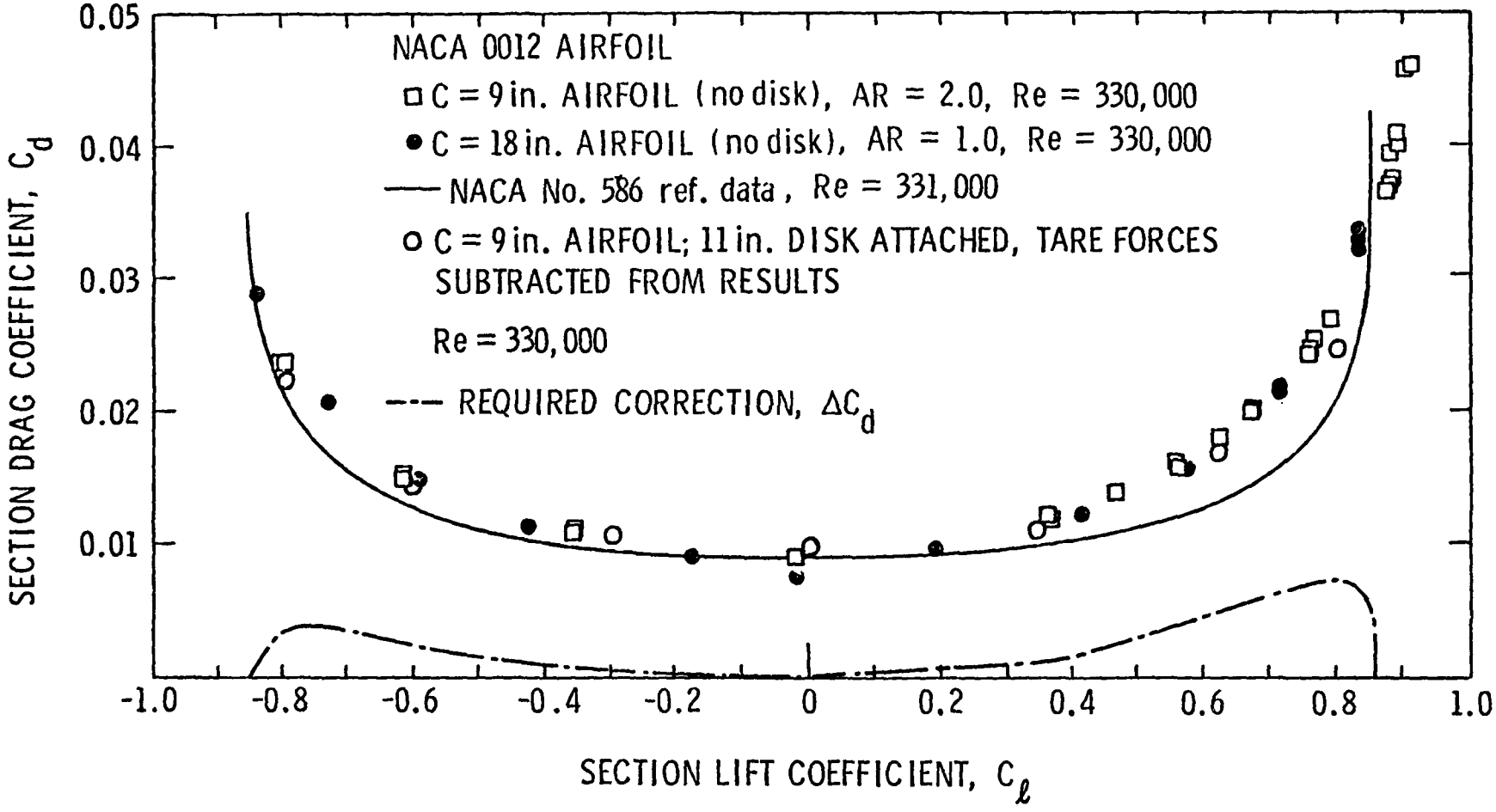

Figure 4. ARL/PSU drag polar (traditional corrections only applied) for c = 9.0 in (228.6 mm) and c = 18.0 (457.2 mm) airfoils without disks. Also shown is the value of ΔC_d required to correct the ARL/PSU data to the NACA curve.

25 August 1981
ALT:PPJ:CBC:cag

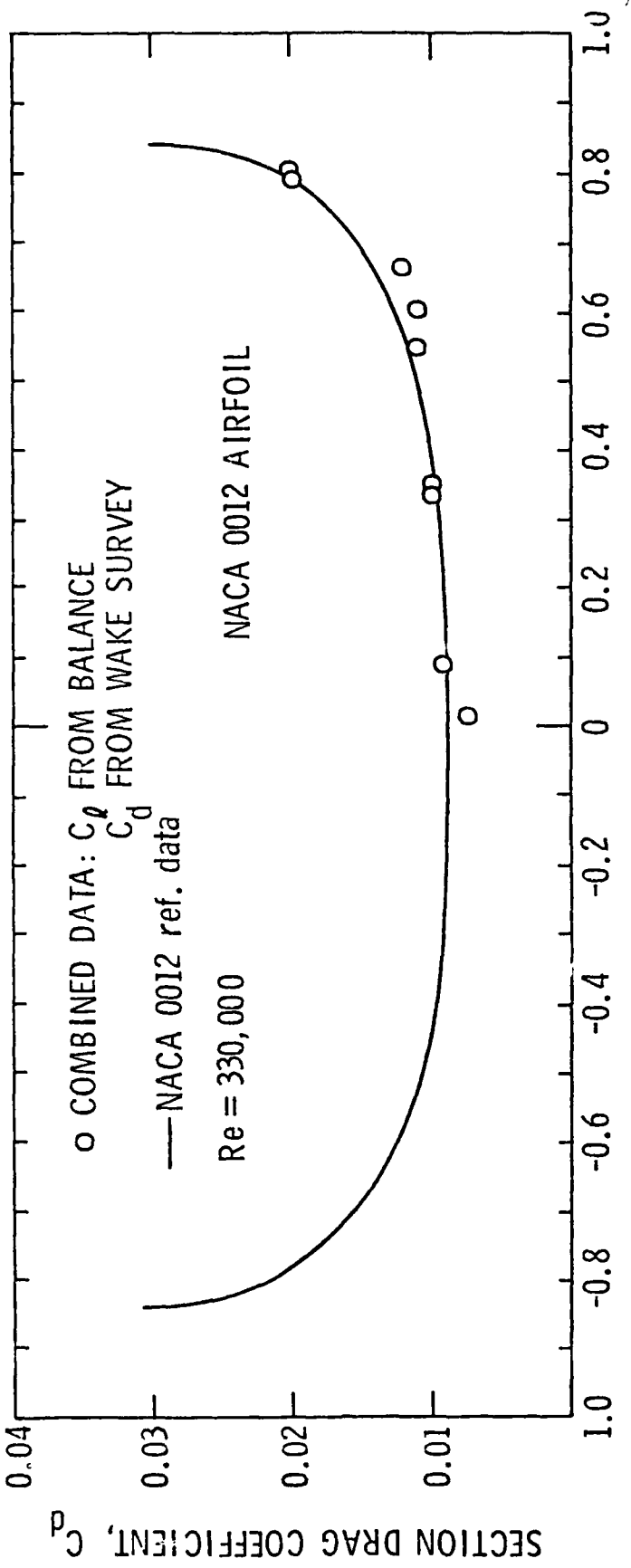

Figure 5. Comparison of NACA data with ARL/PSU C_ℓ and C_d data measured by different techniques.

APPLIED RESEARCH LABORATORY, FLUIDS ENGINEERING DEPARTMENT (USA)
THE PENNSYLVANIA STATE UNIVERSITY
P. O. BOX 30, STATE COLLEGE, PA 16801 (814) 865-1741

SUBSONIC WIND TUNNEL 1953

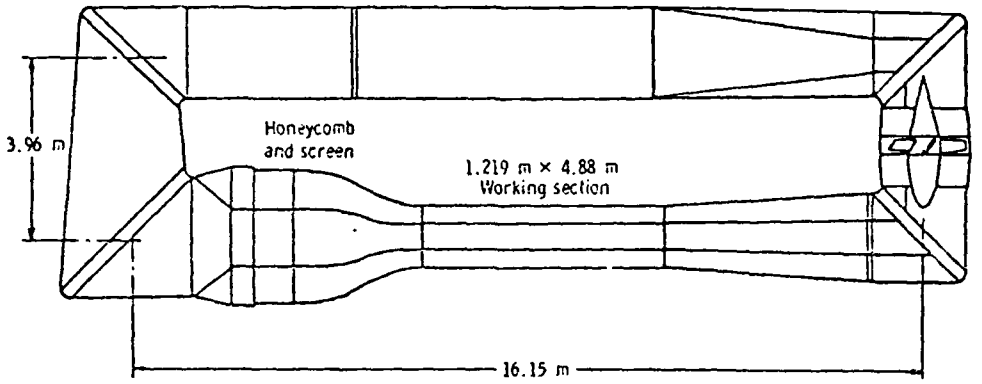

DESCRIPTION OF FACILITY:	Closed Circuit
TYPE OF DRIVE SYSTEM:	Axial-Flow Blower Variable-Speed
TOTAL MOTOR POWER:	150 HP (111.8 kw)
WORKING SECTION MAX. VELOCITY:	45.72 m/s

INSTRUMENTATION: Automatic scanning and rotating mechanisms, pressure sensors, hot-wires

TURBULENCE LEVEL: 0.2 percent

PROPELLER OR MODEL SIZE RANGE: Up to 635.0 mm dia.

TESTS PERFORMED: Pressure distributions over hydrodynamic shapes. Velocity profiles in propeller planes. Hot-wire measurements. Wall interaction effects on hydrofoils.

OTHER REMARKS: The tunnel is subsonic. It is used for basic and applied research. It is well instrumented for the measurement of model boundary layers and their wake turbulence.

PUBLISHED DESCRIPTION: ARL/PSU Report NORD 16597-56, Lehman, 1959

Figure 6. ARL/PSU subsonic wind tunnel.

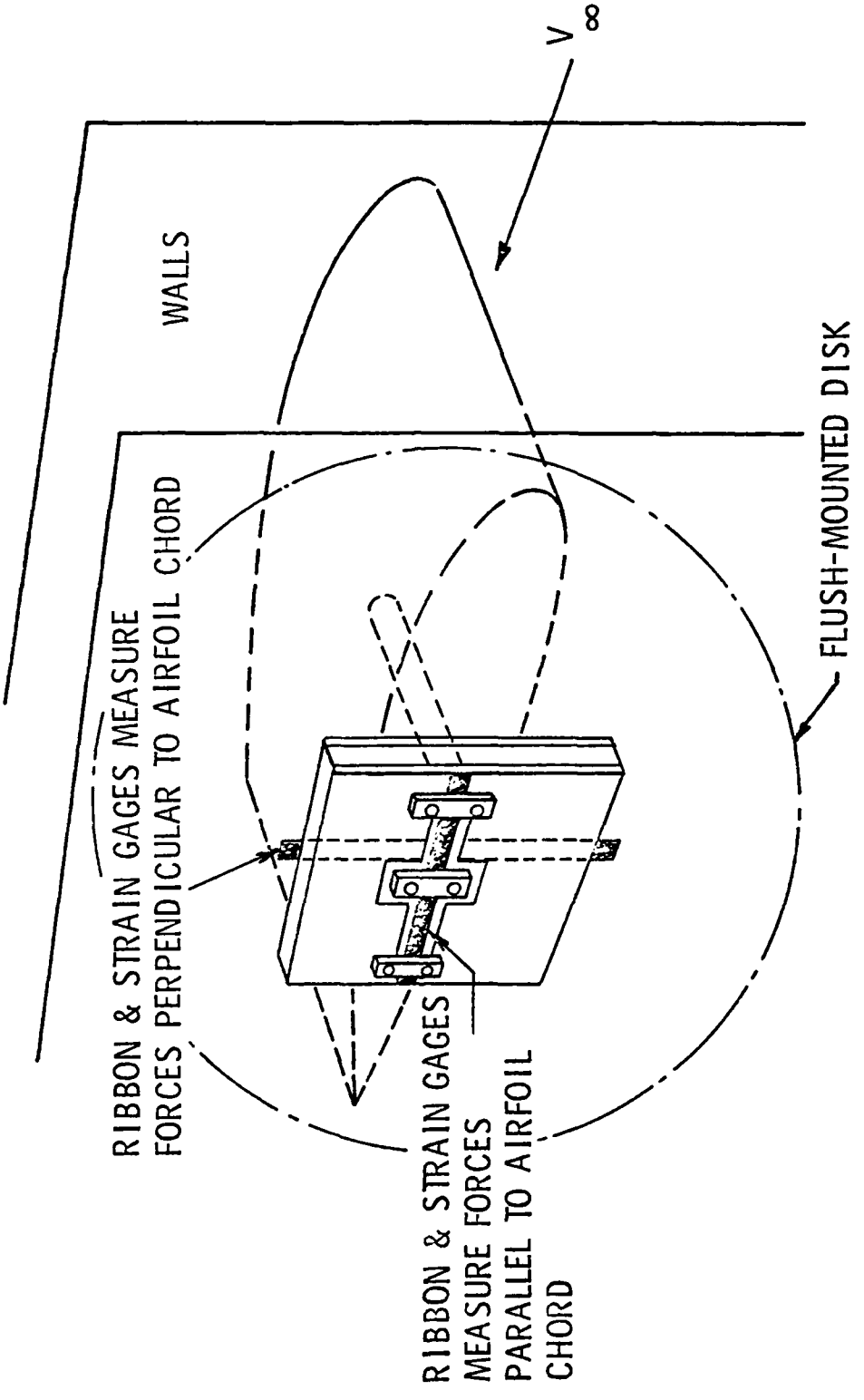

Figure 7. ARL/PSU two-component, cantilevered force balance which rotates with the airfoil.

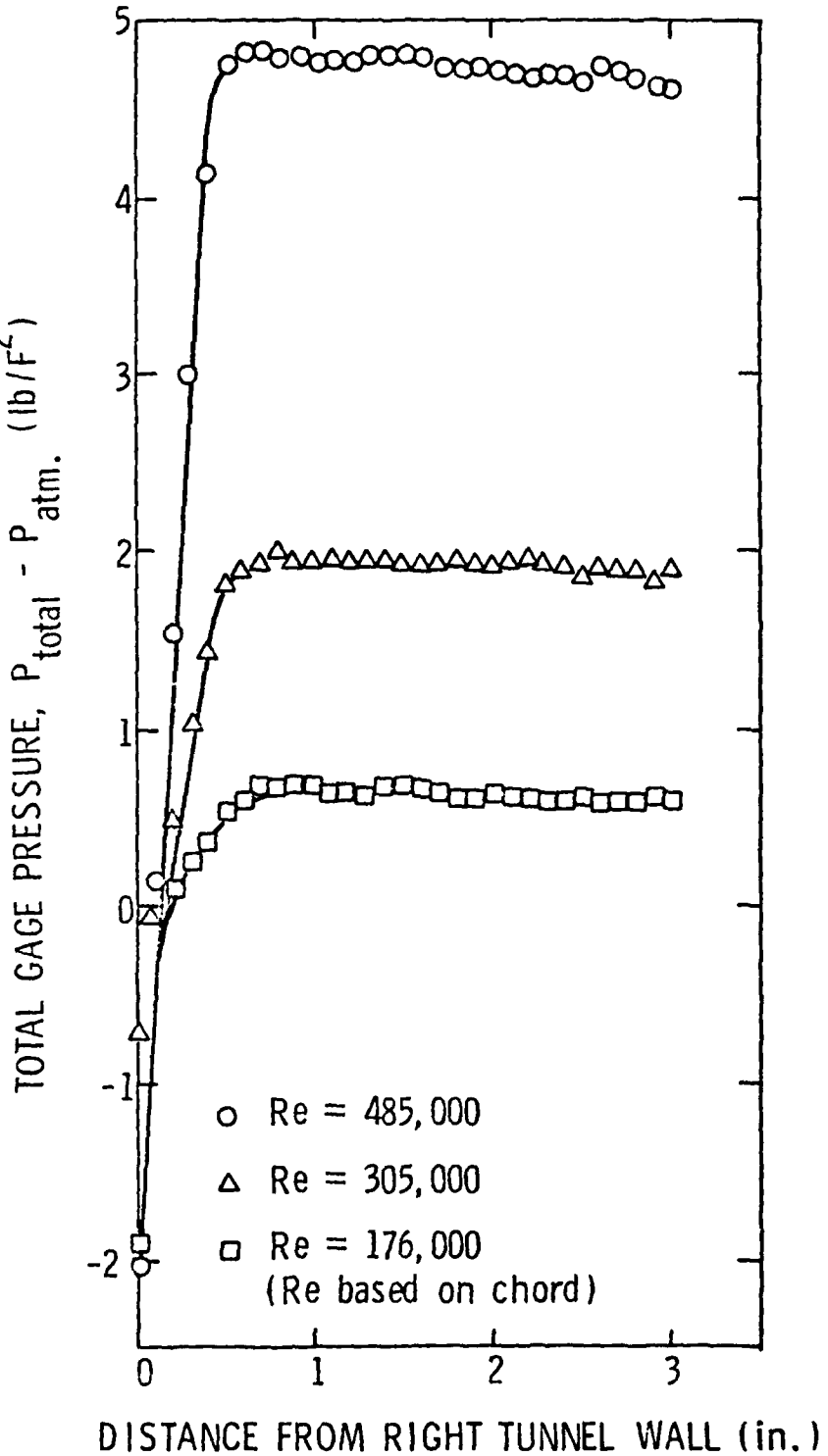

Figure 8. Boundary layer surveys at the balance shaft location.

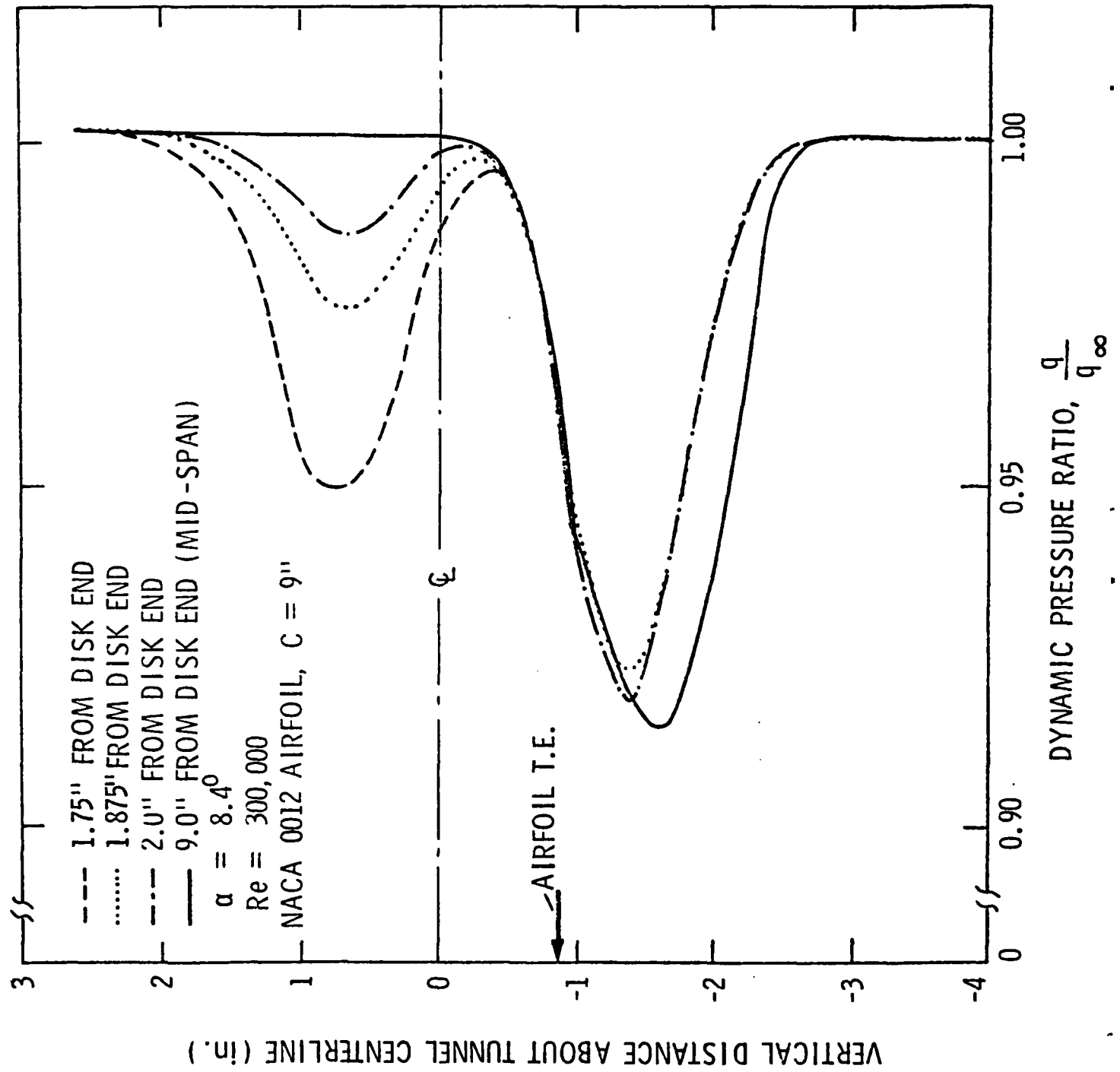

Figure 9. Wake profiles in the vicinity of the airfoil-disk intersection showing the growth of a second wake behind airfoil upper surface.

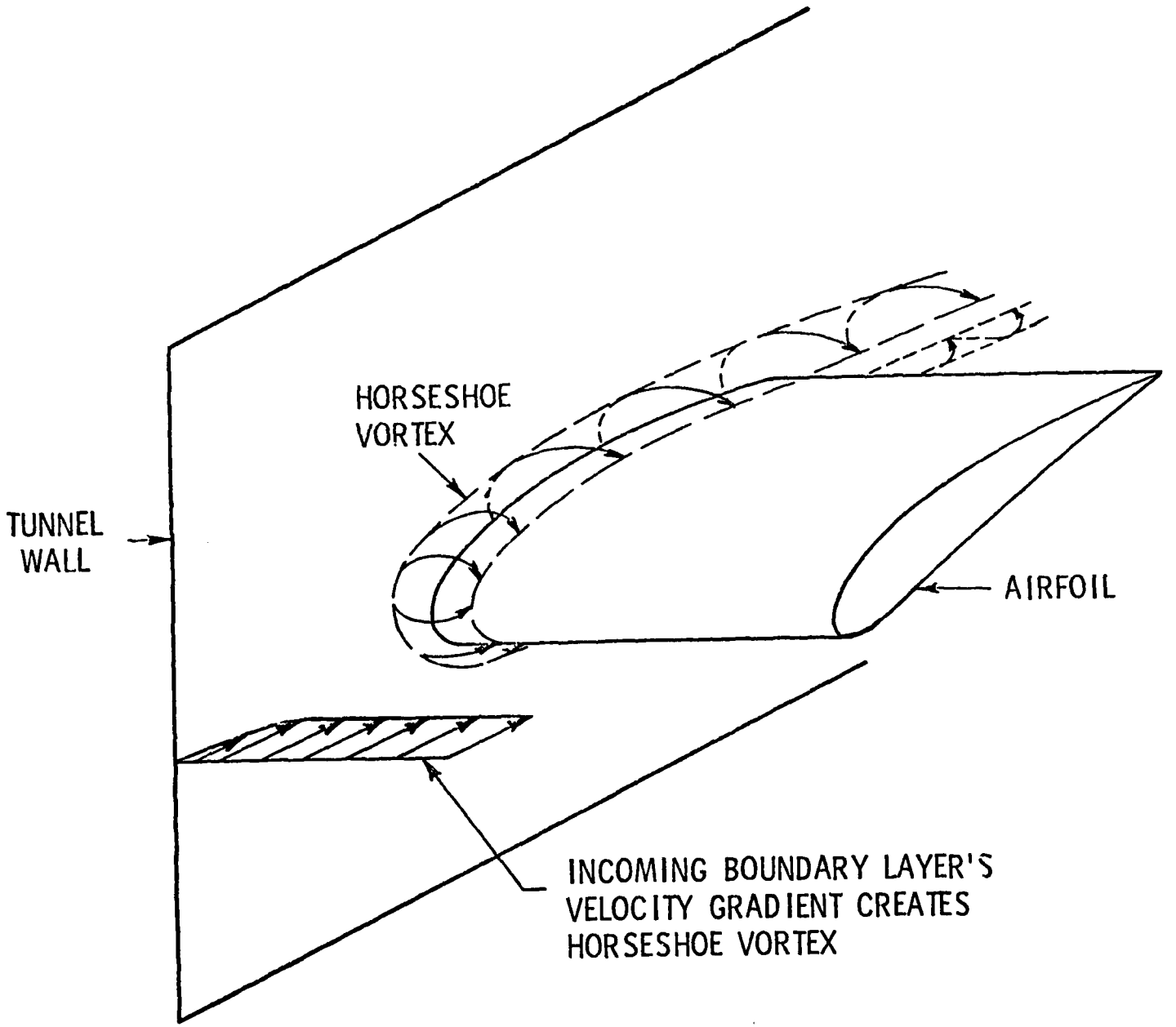

Figure 10. Horseshoe vortex created by the interaction of the velocity gradient and curved airfoil surface at the wall intersection.

25 August 1981
ALT:PRJ:CRG:cag

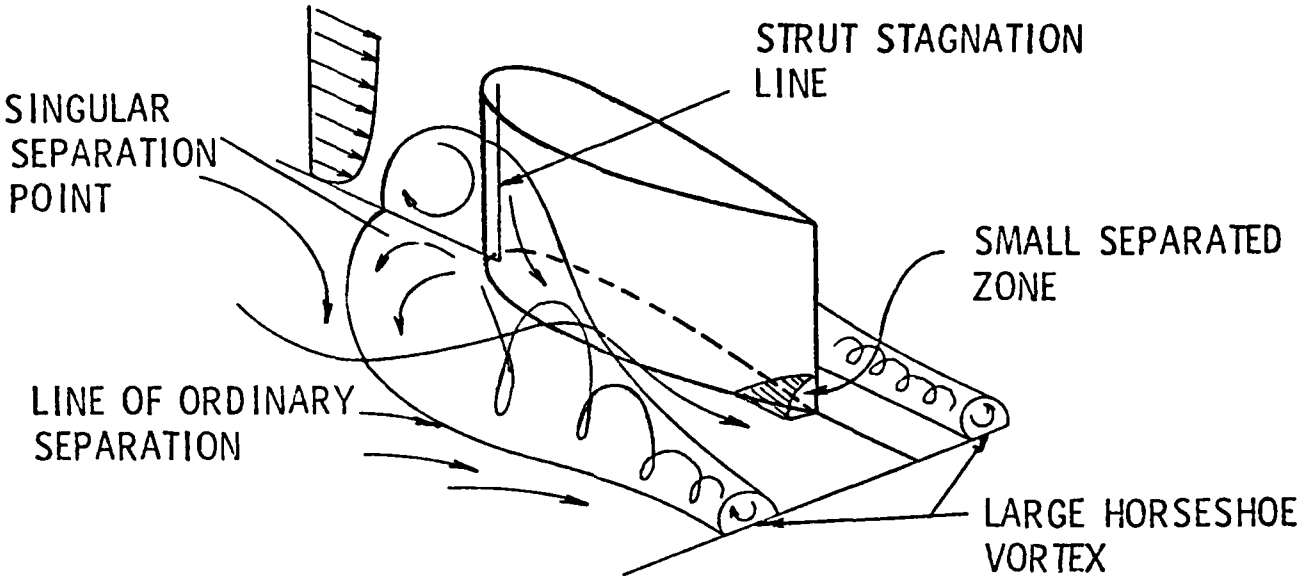

PROPOSED MODEL OF THICK BOUNDARY-LAYER-STRUT INTERACTION

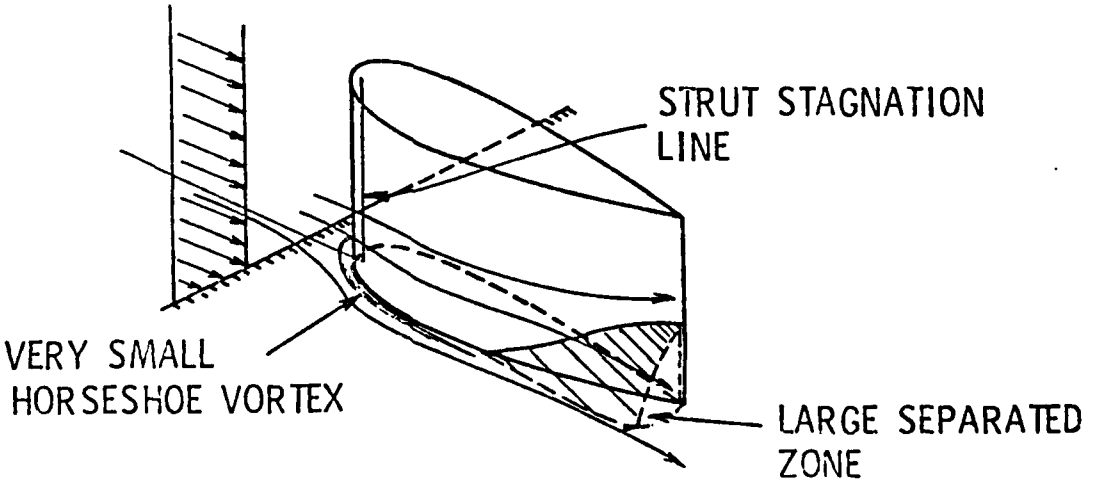

PROPOSED MODEL OF THIN BOUNDARY-LAYER-STRUT INTERACTION

Figure 11. Barber's model for the flow conditions occurring in the vicinity of an airfoil-tunnel wall intersection.

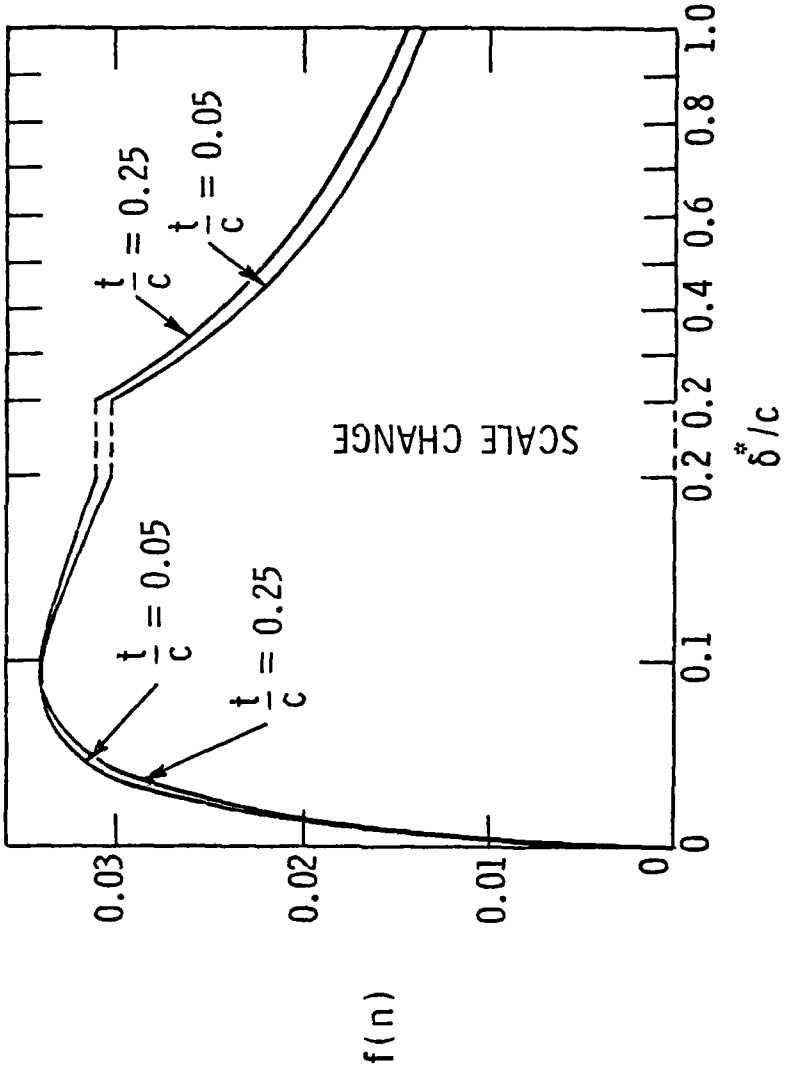

Figure 12. Hawthorne's plot of the variation of f(n) with δ^*/c (Equation 2) for t/c = 0.05 and 0.25.

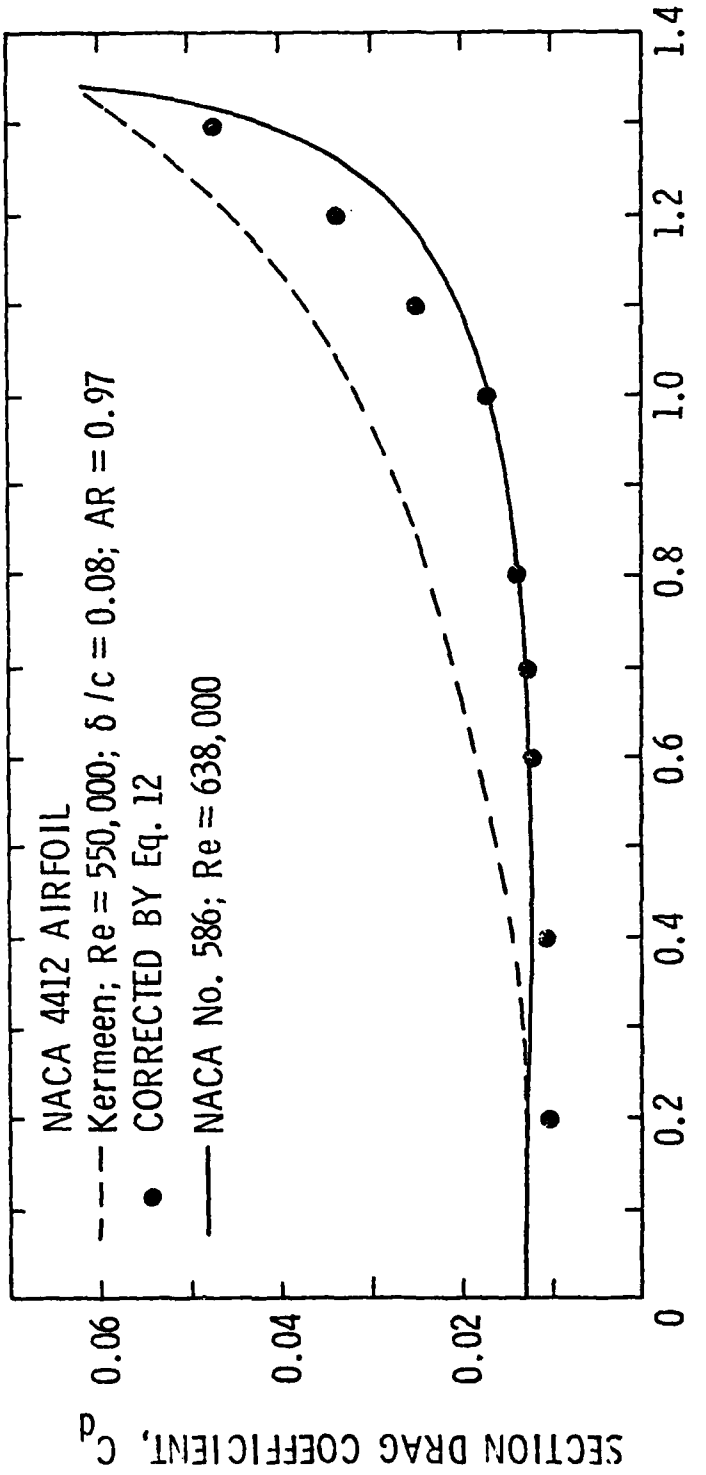

Figure 13. Kermeen's data corrected by Equation (12).

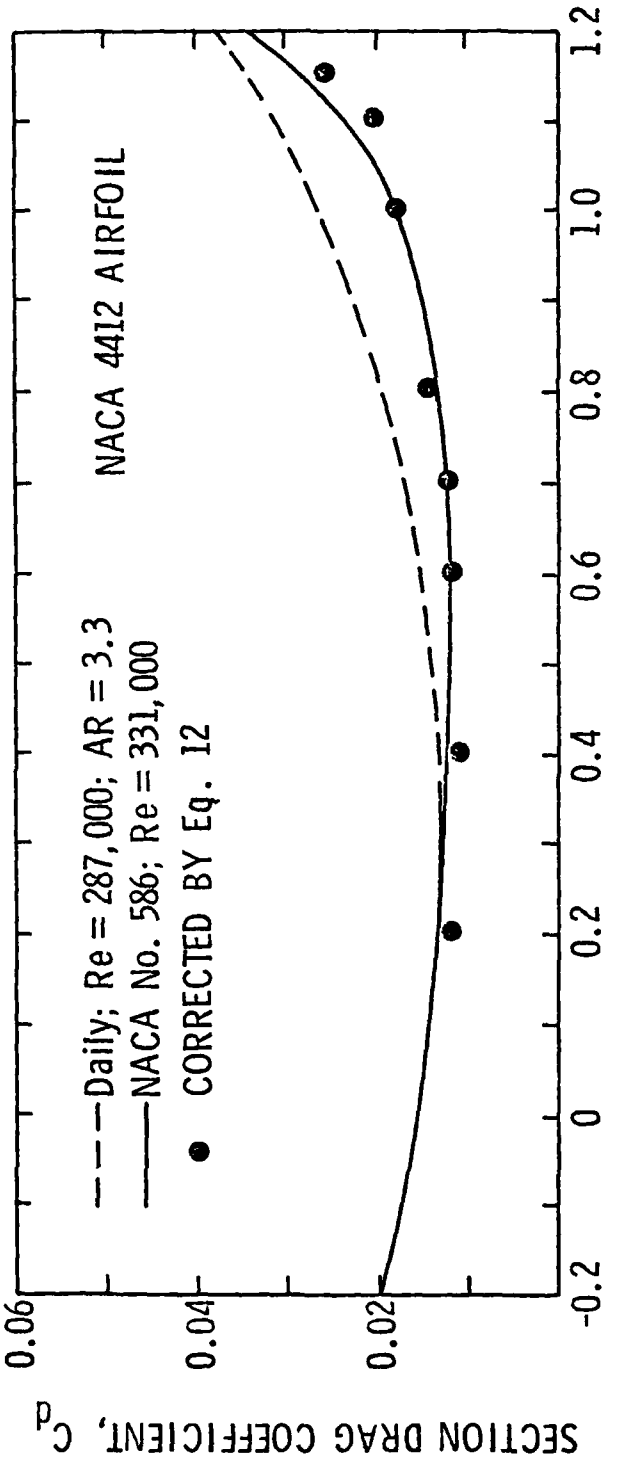

Figure 14. Daily's data corrected by Equation (12).

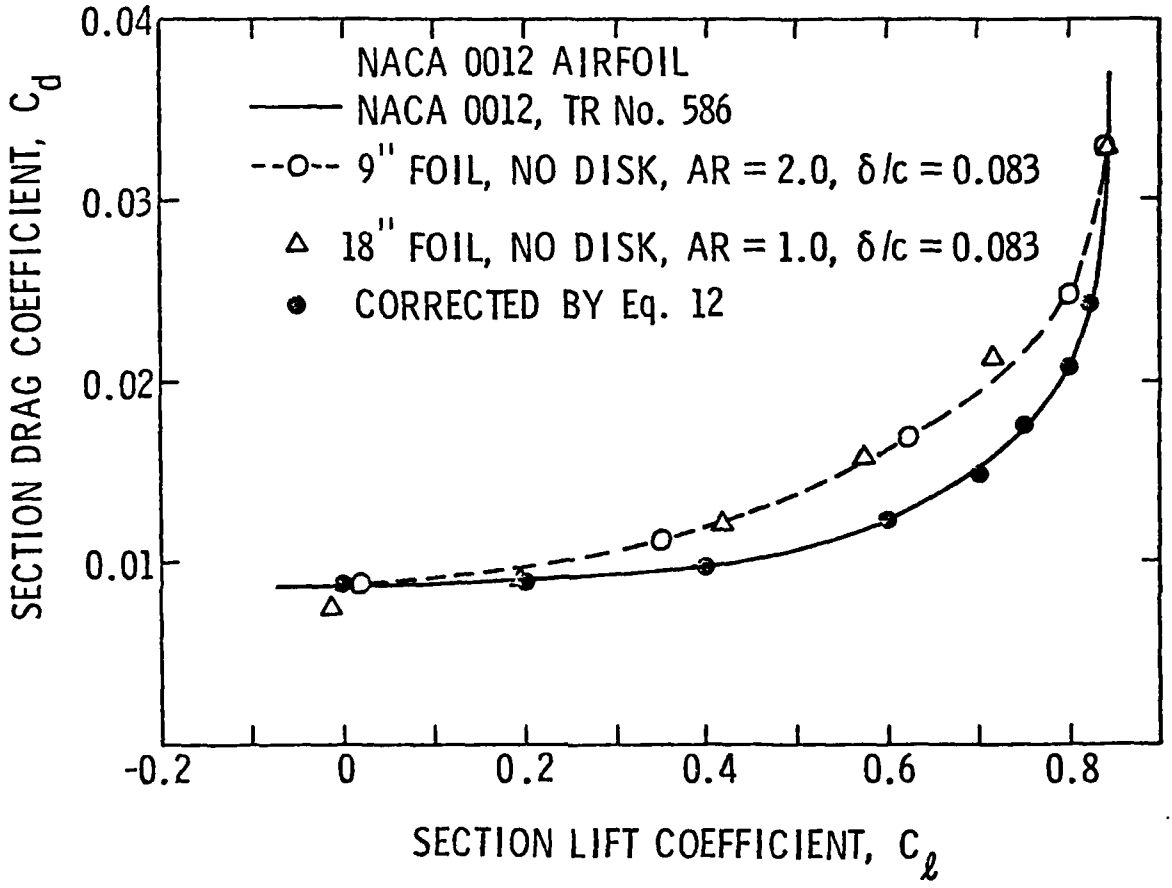

Figure 15. ARL/PSU results corrected by Equation (12).

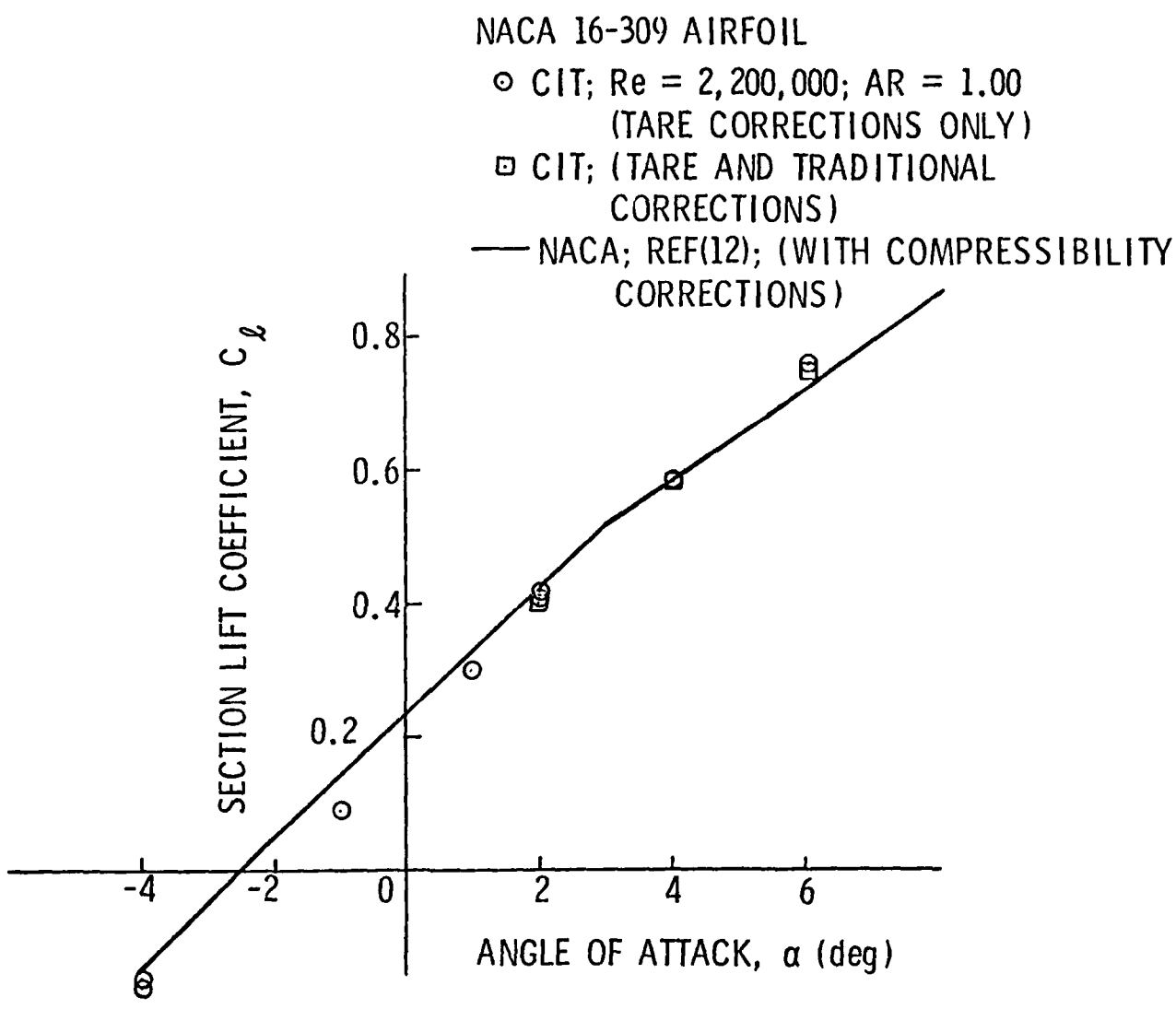

Figure 16. Data measured by Ward at CIT (Reference [8]) on a 6.0 in (152.4 mm) chord NACA 16-309 hydrofoil in the High Speed Water Tunnel

25 August 1981
ALT:RDJ:CRC:cag

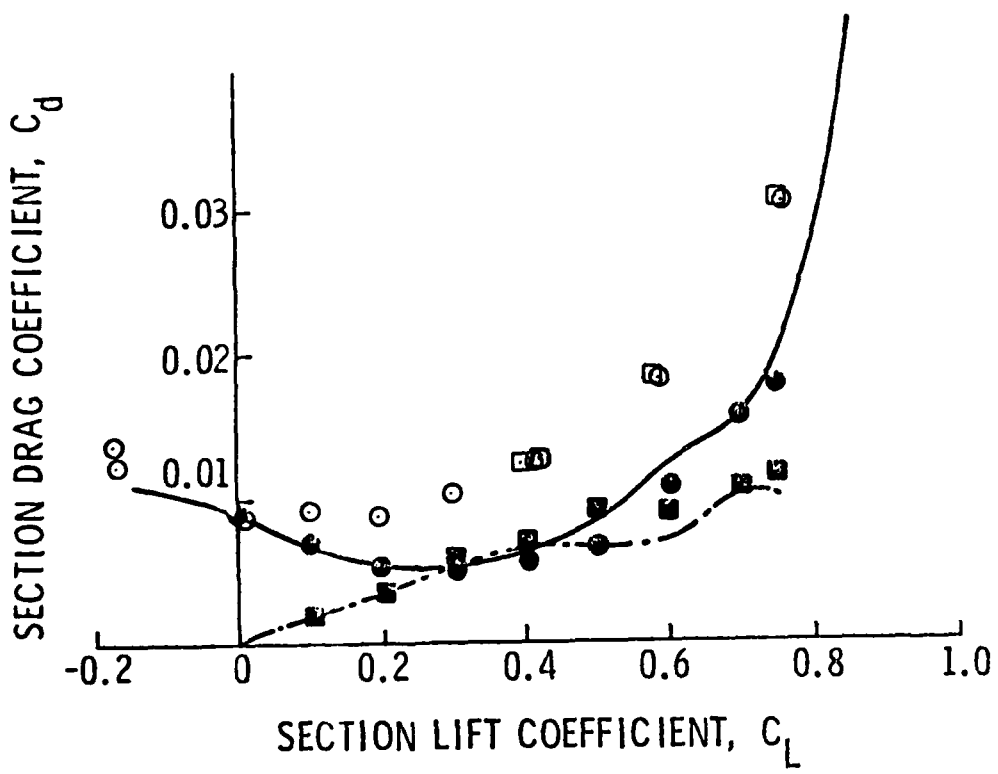

NACA 16-309 AIRFOIL

- ○ CIT; Re = 2,200,000; AR = 1.0 (TARE CORRECTIONS ONLY)
- □ CIT; (TARE AND TRADITIONAL CORRECTIONS)
- —— NACA; REF(12) (WITH COMPRESSIBILITY CORRECTIONS)
- —·— REQUIRED CORRECTION, ΔC_d
- ■ ΔC_d COMPUTED BY Eq. (12)
- ● CIT DATA CORRECTED BY Eq. (12)

Figure 17. CIT drag polar corrected by Equation (12).

DISTRIBUTION LIST FOR UNCLASSIFIED TM 81-176 by A. L. Treaster, P. P. Jacobs, Jr., and G. B. Gurney, dated 25 August 1981.

Commander
Naval Sea Systems Command
Department of the Navy
Washington, DC 20362
Attn: Library
Code NSEA-09G32
(Copy Nos. 1 and 2)

Naval Sea Systems Command
Attn: T. E. Peirce
Code NSEA-63R3
(Copy No. 3)

Commanding Officer
Naval Underwater Systems Center
Newport, RI 02840
Attn: Library
Code 54
(Copy No. 4)

Naval Underwater Systems Center
Attn: R. H. Nadolink
Code 3634
(Copy No. 5)

Commanding Officer
Naval Ocean Systems Center
San Diego, CA 92152
Attn: D. Nelson
Code 6342
(Copy No. 6)

Naval Ocean Systems Center
Attn: M. M. Reischman
Code 2542
(Copy No. 7)

Commander
David W. Taylor Naval Ship R&D Center
Department of the Navy
Bethesda, MD 20084
Attn: W. B. Morgan
Code 154
(Copy No. 8)

David W. Taylor Naval Ship R&D Center
Attn: Y. T. Shen
Code 1524
(Copy No. 9)

David W. Taylor Naval Ship R&D Center
Attn: R. W. Brown
Code 1942
(Copy No. 10)

David W. Taylor Naval Ship R&D Center
Attn: Library
Code 522
(Copy No. 11)

Officer-in-Charge
David W. Taylor Naval Ship R&D Center
Department of the Navy
Annapolis Laboratory
Annapolis, MD 21402
Attn: E. R. Quandt
Code 272
(Copy No. 12)

David W. Taylor Naval Ship R&D Center
Attn: J. G. Stricker
Code 2721
(Copy No. 13)

Commander
Naval Surface Weapons Center
Silver Spring, MD 20910
Attn: J. L. Baldwin
Code WA-42
(Copy No. 14)

Office of Naval Research
Department of the Navy
800 N. Quincy Street
Arlington, VA 22217
Attn: R. D. Cooper
Code 438
(Copy No. 15)

Defense Technical Information Center
5010 Duke Street
Cameron Station
Alexandria, VA 22314
(Copy Nos. 16 through 21)

National Bureau of Standards
Aerodynamics Section
Washington, DC 20234
Attn: P. S. Klebanoff
(Copy No. 22)

Naval Research Laboratory
Washington, DC 20390
Attn: R. J. Hansen
(Copy No. 23)

NASA Lewis Research Center
21000 Brookpark Road
Cleveland, OH 44135
Attn: M. J. Hartmann
MS 5-9
(Copy No. 24)

DISTRIBUTION LIST FOR UNCLASSIFIED TM 81-176 by A. L. Treaster, P. P. Jacobs, Jr., and G. B. Gurney, dated 25 August 1981.

NASA Lewis Research Center
Attn: W. M. McNally
MS 5-9
(Copy No. 25)

NASA Lewis Research Center
Attn: N. C. Sanger
MS 5-9
(Copy No. 26)

California Institute of Technology
Jet Propulsion Laboratory
48000 Oak Grove Drive
Pasadena, CA 91109
Attn: Dr. L. Mack
(Copy No. 27)

Rand Corporation
1700 Main Street
Santa Monica, CA 90406
Attn: C. Gazley
(Copy No. 28)

Dr. Peter van Oossanen
Netherlands Ship Model Basin
Haagsteeg 2
P. O. Box 28
67 AA Wageningen
The Netherlands
(Copy No. 29)

Carl-Anders Johnsson
Statens Skeppsprovningsanstalt
Box 24001
S-400 22 Goteborg
Sweden
(Copy No. 30)

Dr. Ir. A. De Bruijn
Technisch Physische Dienst TNO-TH
Stieltjesweg 1
Postbus 155
Delft
The Netherlands
(Copy No. 31)

Dr. Allen Moore
Admiralty Research Laboratory
Teddington, Middlesex
England
(Copy No. 32)

J. Lewis
University of Newcastle
Newcastle
England
(Copy No. 33)

Dr. John H. Horlock
Vice Chancellor
University of Salford
Salford, M5 4WT
England
(Copy No. 34)

Von Karman Institute for Fluid Dynamics
Turbomachinery Laboratory
Rhode-Saint-Genese
Belgium
Attn: Library
(Copy No. 35)

Dr. D. S. Thompson
Turbine Research Department
Rolls Royce Ltd.
P. O. Box 31
Derby
England
(Copy No. 36)

Whittle Turbomachinery Laboratory
Madingley Road
Cambridge, England
Attn: Sir William Hawthorne
(Copy No. 37)

Whittle Turbomachinery Laboratory
Attn: Dr. D. S. Whitehead
(Copy No. 38)

Professor R. E. Peacock
School of Mechanical Engineering
Cranfield Institute of Technology
Cranfield, Bedford MK430AL
England
(Copy No. 39)

Professor J. P. Gostelow
School of Mechanical Engineering
NSW Institute of Technology
Broadway, Sidney
Australia
(Copy No. 40)

DISTRIBUTION LIST FOR UNCLASSIFIED TM 81-176 by A. L. Treaster, P. P. Jacobs, Jr., and G. B. Gurney, dated 25 August 1981.

Dr. V. H. Arakeri
Department of Mechanical Engineering
Indian Institute of Science
Bangalore 560 012
India
(Copy No. 41)

Institute of High Speed Mechanics
Tohoku University
Sendai
Japan
(Copy No. 42)

Dr. Allan J. Acosta
California Institute of Technology
Division of Engineering for
Applied Sciences
Pasadena, CA 91109
(Copy No. 43)

Professor Patrick Leehey
Department of Ocean Engineering
Room 5-222
Massachusetts Institute of Technology
77 Massachusetts Avenue
Cambridge, MA 02139
(Copy No. 44)

Dr. John L. Lumley
Sibley School of Mechanical and
Aeronautical Engineering
Upson Hall
Cornell University
Ithaca, NY 14850
(Copy No. 45)

Calspan Corporation
4455 Genessee Street
Buffalo, NY 14221
Attn: Head Librarian
(Copy No. 46)

Dr. G. K. Serovy
Mechanical Engineering Department
Iowa State University
Ames, Iowa 50010
(Copy No. 47)

Superintendent (Code 1424)
Naval Postgraduate School
Monterey, CA 93940
(Copy No. 48)

Iowa Institute of Hydraulic Research
The University of Iowa
Iowa City, Iowa 52240
(Copy No. 49)

Dr. Roger E. A. Arndt
St. Anthony Falls Hydraulic Laboratory
University of Minnesota
Mississippi River at 3rd Ave., S.E.
Minneapolis, MN 55414
(Copy No. 50)

Defense Advanced Research Projects Agency
1400 Wilson Boulevard
Arlington, VA 22209
Attn: P. Selwyn, TTO
(Copy No. 51)

Hydronautics, Inc.
Pindell School Road
Laurel, MD 20810
(Copy No. 52)

M. Mackay
Defense Research
Establishme Atlantic
P.O. Box 1012
Dartmouth, Nova Scotia
CANADA B2Y 327
(Copy No. 53)

The Pennsylvania State University
Applied Research Laboratory
P. O. Box 30
State College, PA 16801
Attn: G. B. Gurney
(Copy No. 54)

Applied Research Laboratory
Attn: A. L. Treaster
(Copy No. 55)

Applied Research Laboratory
Attn: G. C. Lauchle
(Copy No. 56)

Applied Research Laboratory
Attn: B. R. Parkin
(Copy No. 57)

Applied Research Laboratory
Attn: GTWT Files
(Copy No. 58)